

Neutrino Physics

Neutrino Propagation in Quantum Field Theory at Short and Long Baselines

V.A. Naumov^{1,*} and D.S. Shkirmanov^{1,†}¹*Joint Institute for Nuclear Research, Laboratory of Theoretical Physics*

(Received xx.xx.2025; Revised xx.xx.2025; Accepted xx.xx.2025)

In a quantum field approach to neutrino oscillations, the neutrino is treated as a propagator, while the external initial and final particle states are described by covariant wave packets. For the asymptotic behavior on short and long macroscopic baselines, the wave packet modified neutrino propagator is expressed through asymptotic series in powers of dimensionless Lorentz and rotation invariant variables. In both regimes, leading-order corrections violate the classical inverse-square law and lead to a decrease in the neutrino-induced event rate. The possibility that the so-called reactor antineutrino anomaly can, at least partially, be explained within this approach is discussed.

PACS numbers: 11.25.Db; 12.15.Ji; 13.15.+g; 14.60.Lm; 14.60.Pq; 28.50.Dr; 29.85.Ca; 29.85.Fj

Keywords: Neutrino, Quantum Field Theory, Wave packet, Inverse square law violation

1. INTRODUCTION

Numerous inconsistencies in the standard quantum-mechanical theory of neutrino oscillations led to the development of a more consistent approach based on the S-matrix formalism of quantum field theory (QFT) [1]. Over the past decades, a number of studies have been devoted to elaborating this approach; a list of these studies can be found, e.g., in Ref. [2]. The present study is based on the formalism developed in Refs. [3, 4]. Let's briefly recall its key ingredients.

Within the standard “plane wave” (PW) *S*-matrix formalism, single-particle states are defined as Fock states, $|\mathbf{k}, s\rangle = \sqrt{2E_{\mathbf{k}}} a_{\mathbf{k}s}^\dagger |0\rangle$ ($E_{\mathbf{k}}^2 = |\mathbf{k}|^2 + m^2$), which contain no information about the particle's space-time location and cannot be used to describe the oscillation phenomenon [2–4]. To account for coordinate dependence, we can use wave-packet (WP) states, which are simply covariant linear superpositions of Fock states:

$$|\mathbf{p}, s, x\rangle = \int \frac{d\mathbf{k} \phi(\mathbf{k}, \mathbf{p}) e^{i(\mathbf{k}-\mathbf{p})x}}{(2\pi)^3 2E_{\mathbf{k}}} |\mathbf{k}, s\rangle, \quad (1)$$

where $\phi(\mathbf{k}, \mathbf{p})$ is a model-dependent scalar function that determines the WP shape and (“correspondence principle”) transforms into the normalized 3D Dirac δ function in the PW limit: $\phi(\mathbf{k}, \mathbf{p}) \rightarrow (2\pi)^3 2E_{\mathbf{p}} \delta(\mathbf{k}-\mathbf{p})$. The amplitude is constructed as the standard QFT amplitude, $\langle \text{out} | \mathbb{S} | \text{in} \rangle \langle \text{in} | \text{in} \rangle \langle \text{out} | \text{out} \rangle^{-1/2}$, where **in** and **out** states are, in general, multi-WP states. The amplitude depends on the space-time coordinates of all WPs ($\in |\text{in}\rangle$ and $|\text{out}\rangle$), which interact in the macroscopically separated vertices of a Feynman diagram – “source” and “detector” (see Fig. 1 in Sect. 3). Due to the localised WP states, the amplitude is suitable to describe the processes that depend on the macroscopic spatial and temporal intervals between the vertices.

2. RELATIVISTIC GAUSSIAN PACKET

For our purposes, we use the so-called relativistic Gaussian packet (RGP) model [4], in which the “form factor” function $\phi(\mathbf{k}, \mathbf{p})$ in Eq. (1) has the form

$$N_\sigma \exp \left[\frac{(E_{\mathbf{k}} - E_{\mathbf{p}})^2 - (\mathbf{k} - \mathbf{p})^2}{4\sigma^2} \right] \equiv \phi_G(\mathbf{k}, \mathbf{p}).$$

Here σ is the momentum spread (dispersion) of RGP and the normalization constant N_σ is obtained from the linear normalization condition

$$\int \frac{d\mathbf{k} \phi_G(\mathbf{k}, \mathbf{p})}{(2\pi)^3 2E_{\mathbf{k}}} = 1;$$

This is a technical point, but it is useful and fully consistent with the correspondence principle. The coordinate representation of RGP,

$$\psi_G(\mathbf{p}, x) = \int \frac{d\mathbf{k}}{(2\pi)^3 2E_{\mathbf{k}}} \phi_G(\mathbf{k}, \mathbf{p}) e^{i\mathbf{k}x},$$

can be approximately written as

$$\psi_G(\mathbf{p}, x) = \exp \left\{ i(px) - \frac{\sigma^2}{m^2} [(px)^2 - m^2 x^2] \right\}$$

(so-called “contracted” RGP or CRGP), which is valid under two invariant conditions: $(px)^2 \ll m^4/\sigma^4$ and $(px)^2 - m^2 x^2 \ll m^4/\sigma^4$. It's easy to see that $|\psi_G|$ does not depend on time in the proper reference frame. In this study, we will use exactly this approximation.

3. THE PROCESS UNDER STUDY

Figure 1 shows a generic macroscopic Feynman diagram describing the class of processes under consideration. Here X_s and X_d denote macroscopically separated regions in space and time in which intermediate neutrinos are produced and detected, respectively. $I_{s,d}$

* E-mail: vnaumov@theor.jinr.ru

† E-mail: dmitry@shkirmanov.com

denote initial particles (WPs) at the source and detector vertices, respectively; $F_{s,d}$ and $F'_{s,d}$ denote the sets of final WPs (the notation is clear from the figure). The “oscillations” (= flavor transitions) arise from the

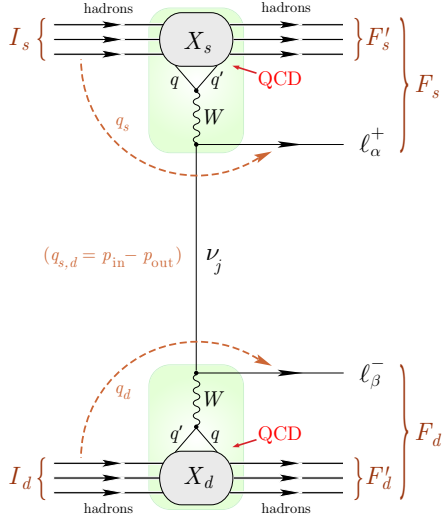


Figure 1. Macroscopic Feynman diagram representing the process under discussion. Initial and final states in source and detector vertices are wave packets. Notations are explained in the text. For details, see Ref. [2].

interference of the Feynman diagrams with different mass (virtual) eigenfields ν_j ($j = 1, 2, 3$) in the intermediate states. In other words, in this formalism, neutrino oscillations are the result of interference, not mixing. The amplitude of the process is determined by the Lagrangian of the Standard Model, extended to include neutrino masses:

$$\mathcal{L}_W(x) = -\frac{g}{2\sqrt{2}} [j_\ell(x)W(x) + j_q(x)W(x) + \text{H.c.}] .$$

Here g is $SU(2)$ coupling constant; $j_\ell(x)$ and $j_q(x)$ are the lepton and quark weak charged currents:

$$\begin{aligned} j_\ell^\mu(x) &= \sum_{\alpha i} V_{\alpha i}^* \bar{\nu}_i(x) \gamma^\mu (1 - \gamma_5) \ell_\alpha(x), \\ j_q^\mu(x) &= \sum_{qq'} V_{qq'}^* \bar{q}(x) \gamma^\mu (1 - \gamma_5) q'(x). \end{aligned}$$

Here $\alpha = e, \mu, \tau$, $i = 1, 2, 3$, $q = u, c, t$, $q' = d, s, b$, $V_{\alpha i}$ and $V_{qq'}$ are elements of the neutrino and quark mixing matrices (PMNS and CKM), respectively; $\ell_\alpha(x)$ are the lepton field, $q(x)$ and $q'(x)$ are the quark fields. For our aims, we retain only the leading non-vanishing term of the perturbation theory.

4. INVERSE SQUARE LAW VIOLATION

It can be shown that space-time dependence of the amplitude is defined by the neutrino propagator modified by the external WPs:

$$J(X) = \int \frac{d^4 q}{(2\pi)^4} \frac{\tilde{\delta}_s(q - q_s) \tilde{\delta}_d(q + q_d) (\hat{q} + m) e^{-iqX}}{q^2 - m^2 + i\epsilon}. \quad (2)$$

Here $\tilde{\delta}_{s,d}$ are the “smeared” δ -functions responsible for approximate 4-momentum conservation at the source and detector vertices, $X = (T, \mathbf{L})$ is the space-time separation between the source and detector vertices; $q_{s,d}$ are the 4-momentum transfers at the source/detector; and m ($\equiv m_j$) is the neutrino mass.

Integral (2) was studied in detail in two opposite asymptotic regimes: short baselines [5] ($1/\Sigma_{\text{SBL}}^2 \ll L^2 \ll |\mathbf{q}|^2/\Sigma_{\text{SBL}}^4$) and long baselines [6] ($L^2 \gg |\mathbf{q}|^2/\Sigma_{\text{LBL}}^4$), where Σ_{SBL} and Σ_{LBL} are the effective momentum scales for the short and long baseline asymptotics, respectively. These scales are defined by the momentum spreads σ_ν , masses m_ν , and momenta \mathbf{p}_ν of all **in** and **out** WPs $\nu \in I_s \oplus I_d \oplus F_s \oplus F_d$ in the diagram in Fig. 1. Since the solutions are quite cumbersome, we will provide only the briefest summaries here. For the SBL asymptotics, the solution is a triple asymptotic series in powers of small invariant parameters dependent of the deeply virtual neutrino 4-momentum and 4-vector X . For the LBL asymptotics, the 3D part (over \mathbf{q}) of the 4D integral (2) can be evaluated using the extended Grimus-Stockinger theorem [6, 7]. The remaining integral over q_0 for the LBL asymptotics can be evaluated using the saddle-point method. Using these solutions, one can show that in the **ultrarelativistic** approximation, the number of neutrino events detected during the detector exposure time τ_d can be (somewhat symbolically) written as

$$\begin{aligned} \tau_d \sum_{\text{spins}} \int d\mathbf{x} \int d\mathbf{y} \int d\mathfrak{P}_s \int d\mathfrak{P}_d \int d|\mathbf{q}| \\ \times \frac{\mathcal{P}_{\alpha\beta}(|\mathbf{q}|, |\mathbf{y} - \mathbf{x}|)}{4(2\pi)^3 |\mathbf{y} - \mathbf{x}|^2} \times (1 - \text{ISLV corrections}). \end{aligned} \quad (3)$$

Here, the differential forms $d\mathfrak{P}_{s,d}$ are defined as

$$\begin{aligned} d\mathfrak{P}_s &= \prod_{a \in I_s} \frac{d\mathbf{p}_a f_a(\mathbf{p}_a, s_a, \mathbf{x})}{(2\pi)^3 2E_a} \\ &\times \prod_{b \in F_s} \frac{d\mathbf{p}_b}{(2\pi)^3 2E_b} (2\pi)^4 \delta_s(q - q_s) |M_s|^2, \\ d\mathfrak{P}_d &= \prod_{a \in I_d} \frac{d\mathbf{p}_a f_a(\mathbf{p}_a, s_a, \mathbf{y})}{(2\pi)^3 2E_a} \\ &\times \prod_{b \in F_d} \frac{[d\mathbf{p}_b]}{(2\pi)^3 2E_b} (2\pi)^4 \delta_d(q + q_d) |M_d|^2; \end{aligned}$$

integrations over \mathbf{x} and \mathbf{y} are performed over the spatial volumes of the source and detector physical devices, respectively; $f_a(\mathbf{p}_a, s_a, \mathbf{x})$ is the distribution function of particles of type a in the source (for $d\mathfrak{P}_s$) and detector (for $d\mathfrak{P}_d$); $E_{a,b}$ are the energies of the corresponding particles; $\delta_{s,d}$ are “smeared” delta functions (not identical to $\tilde{\delta}_{s,d}$) responsible for an approximate energy-momentum conservation in the source and detector, respectively; $M_{s,d}$ are the standard QFT matrix elements describing interaction in the source and detector respectively. Square brackets in $d\mathfrak{P}_d$ indicate that there is no integration over the final particles in the detector. The function $\mathcal{P}_{\alpha\beta}(|\mathbf{q}|, |\mathbf{y} - \mathbf{x}|)$ is a generalization of the QFT oscillation probability, which reproduces the standard quantum mechanical

formula with some modifications that are not essential in the context of this study. The term $|\mathbf{y} - \mathbf{x}|^2$ in the denominator of Eq. (3) accounts for the standard inverse-square law (ISL), which states that the neutrino event rate is proportional to $1/L^2$, where $L = |\mathbf{L}|$ is the distance between the source and detector devices. Finally, the “ISLV corrections” in Eq. (3) denotes the asymptotic expansion that depends on $|\mathbf{x} - \mathbf{y}|$ and is responsible for the ISL violation (ISLV). In the leading order, these corrections yield the following distance dependence of the event rate for the long and short baselines, respectively:

$$\frac{dN_\nu}{dt} \propto \frac{1}{L^2} \left[1 - \frac{L_0^2}{L^2} + \dots \right], \quad L^2 \gg \frac{E_\nu^2}{\Sigma_{\text{LBL}}^4},$$

$$\frac{dN_\nu}{dt} \propto \frac{1}{L^2} \left[1 - \frac{L^2}{L_0^2} + \dots \right], \quad \frac{1}{\Sigma_{\text{SBL}}^2} \ll L^2 \ll \frac{E_\nu^2}{\Sigma_{\text{SBL}}^4}.$$

Clearly, the factor $1/L^2$ (for both asymptotics) represents the classical ISL and the power corrections in the square brackets violate the ISL. As can be seen, for both regimes, the ISLV corrections decrease the neutrino event rate in the detector. The parameters L_0 and L'_0 define the scales at which the ISLV occurs. The order of magnitude of these parameters can be very roughly estimated as:

$$L_0 \sim L'_0 \sim 20 \left\langle \left(\frac{E_\nu}{1 \text{ MeV}} \right) \left[\frac{\sigma_{\text{eff}}(E_\nu)}{1 \text{ eV}} \right]^{-2} \right\rangle \text{ cm.} \quad (4)$$

Here, $\sigma_{\text{eff}} \sim \Sigma_{\text{SBL}} \sim \Sigma_{\text{LBL}}$ and E_ν is the virtual neutrino energy; the formalism does not formally exclude the possibility that $\Sigma_{\text{SBL}} \gtrsim \Sigma_{\text{LBL}}$. It is clear that the ISLV for reactor antineutrinos can be observed at distances of the order of meters, for reasonable values of the parameter $\sigma_{\text{eff}}(E_\nu)$. In Ref. [8] and in our earlier papers [9], the possibility is discussed that the ISLV could be responsible (at least partly) for the long-standing reactor antineutrino anomaly and maybe for the anomalies in neutrino experiments with the artificial neutrino sources at Ga-Ge solar neutrino detectors (see Ref. [8] and references therein). When the ISLV effects are taken into account, the principal behavior of the neutrino event rate in the detector as a function of distance may appear as symbolically shown in Fig. 2. For both LBL and SBL asymptotics, the theory predicts a neutrino deficit at short distances. The transient regime cannot be described by the two obtained asymptotic expansions and requires a different mathematical analysis.

5. REACTOR EXPERIMENTS AND INVERSE SQUARE LAW VIOLATION

To search for the inverse-square violation effect, we analyzed reactor $\bar{\nu}_e$ experiments. As part of our analysis, we estimated systematic error correlations in the reactor data set. The theoretical model used for the analysis has the following form:

$$T(L; N_0, L_0) = N_0 \cdot \langle P_{\text{surv}}^{3\nu}(L) \rangle \cdot \left(1 - \frac{L_0^2}{L^2} \right). \quad (5)$$

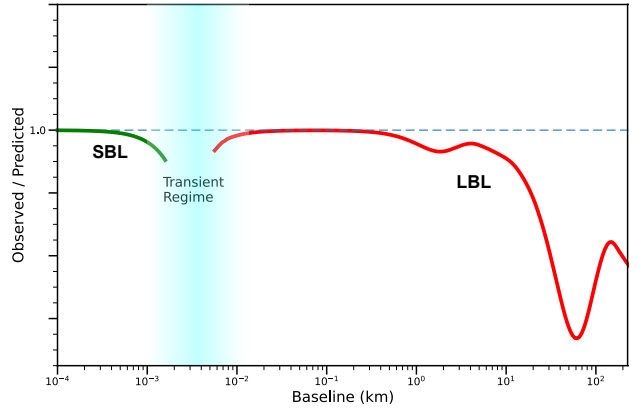


Figure 2. Graphical representation of the ISL effect (observed-to-predicted ratio vs. distance).

Here, L_0 is a free parameter responsible for the inverse-square violation effect, N_0 is a free normalization parameter introduced to account for $\bar{\nu}_e$ flux uncertainty; and

$$\langle P_{\text{surv}}^{3\nu}(L) \rangle = \frac{\int dE \sum_k f_k P_{\text{surv}}^{3\nu}(L, E) \sigma(E) S_k(E)}{\int dE \sum_k f_k \sigma(E) S_k(E)}.$$

Here, f_k is the fraction of the main fissile isotope contributing to the $\bar{\nu}_e$ flux with an energy spectrum $S_k(E)$, $\sigma(E)$ is the IBD cross section [10], and $P_{\text{surv}}^{3\nu}(L, E)$ is the $\bar{\nu}_e$ survival probability in the 3ν mixing scheme:

$$P_{\text{surv}}^{3\nu}(L, E) = 1 - \cos^4 \theta_{13} \sin^2(2\theta_{12}) \sin^2 \Delta_{21} - \sin^2(2\theta_{13}) (\cos^2 \theta_{12} \sin^2 \Delta_{31} + \sin^2 \theta_{12} \sin^2 \Delta_{32}),$$

with $\Delta_{ij} = 1.267 \Delta m_{ij}^2 L/E$. We performed our analysis for different models of $\bar{\nu}_e$ spectra to verify the consistency of the results. Figure 3 shows the fit results for the Kurchatov Institute (KI) $\bar{\nu}_e$ spectrum [11]. The best-fit values of the parameter are shown in the figure. A non-zero best-fit value of the parameter L_0 indicates that the reactor data indeed exhibits a slight ISLV. At the same time, the accuracy of the reactor data does not allow for a reliable determination of the lower bound for the parameter L_0 . Different models (Huber-Mueller [12, 13], Fallot et al. [14]) of $\bar{\nu}_e$ spectra yield similar results: while the best-fit value of N_0 depends significantly on the spectrum model, the best-fit value of L_0 changes only slightly, well within the uncertainties of the analysis. For example, for the Huber-Mueller $\bar{\nu}_e$ spectrum, we obtained the following best-fit parameter values: $N_0 = 0.948^{+0.042}_{-0.039}$, $L_0 = 1.34^{+0.68}_{-1.34}$, $\chi^2/\text{NDF} = 115.5/122$. As can be seen, the N_0 parameter is inconsistent with unity, indicating a discrepancy between the experimental data and the Huber-Mueller spectrum. For the Fallot spectrum, the best-fit parameter values are $N_0 = 1.005^{+0.044}_{-0.041}$, $L_0 = 1.21^{+0.73}_{-1.21}$, $\chi^2/\text{NDF} = 116.9/122$. Clearly, the Fallot spectrum does not require flux normalization.

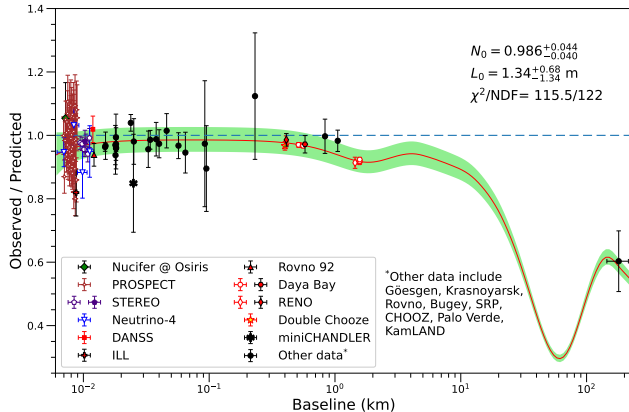


Figure 3. Ratio of observed to predicted rates for the KI $\bar{\nu}_e$ spectrum [11]. Solid line represents the best-fitting theoretical model (5), and the band corresponds to the 68% CL. Filled points represent absolute measurements, and open ones are for the relative measurements normalized to the best-fit curve; references to experiments are given in Ref. [8]. The experimental errors shown do not include the overall normalization uncertainty, which is at least 2.7%.

6. CONCLUSIONS AND DISCUSSION

The QFT approach to neutrino oscillations predicts that the classical inverse-square law could be violated.

The scale at which this violation occurs depends on the momentum spreads of the **in** and **out** wave packets, which are parameters of the theory; therefore, the actual distance at which the ISLV occurs cannot be derived from “first principles”. The available reactor data hint that ISLV has already been observed, but the best-fit value of L_0 is formally compatible with zero. New experiments with intense $\nu/\bar{\nu}$ sources and sectioned or movable detector(s) (such as BEST-2, SOX/CeSOX, CeLAND) are required in order to test the theory.

It is possible that ISLV is also responsible for anomalies in experiments with artificial (anti)neutrino sources as well, although the numerical value of L_0 would differ for these experiments, since L_0 depends on neutrino energy according to Eq. (4). We would also like to add that if new data (e.g., from DANSS) rule out ISLV, it would not mean a confutation of the QFT approach. Rather, it would only indicate that σ_{eff} is above the experimental sensitivity threshold.

7. CONFLICT OF INTEREST

The authors declare that they have no conflicts of interest.

- [1] I. Yu. Kobzarev, B. V. Martemyanov, L. B. Okun, and M. G. Shchepkin, Sum rules for neutrino oscillations, *Yad. Fiz.* **35**, 1210 (1982); C. Giunti, C. W. Kim, and U. W. Lee, When do neutrinos cease to oscillate?, *Phys. Lett. B* **421**, 237 (1998), [arXiv:hep-ph/9709494](https://arxiv.org/abs/hep-ph/9709494); When do neutrinos really oscillate? Quantum mechanics of neutrino oscillations, *Phys. Rev. D* **44**, 3635 (1991); W. Grimus and P. Stockinger, Real oscillations of virtual neutrinos, *Phys. Rev. D* **54**, 3414 (1996), [arXiv:hep-ph/9603430](https://arxiv.org/abs/hep-ph/9603430).
- [2] D. V. Naumov and V. A. Naumov, Quantum field theory of neutrino oscillations, *Phys. Part. Nucl.* **51**, 1 (2020).
- [3] V. A. Naumov and D. V. Naumov, Relativistic wave packets in a field theoretical approach to neutrino oscillations, *Russ. Phys. J.* **53**, 549 (2010).
- [4] D. V. Naumov and V. A. Naumov, A diagrammatic treatment of neutrino oscillations, *J. Phys. G* **37**, 105014 (2010), [arXiv:1008.0306v2 \[hep-ph\]](https://arxiv.org/abs/1008.0306v2).
- [5] V. A. Naumov and D. S. Shkirmanov, Virtual neutrino propagation at short baselines, *Eur. Phys. J. C* **82**, 736 (2022), [arXiv:2208.02621 \[hep-ph\]](https://arxiv.org/abs/2208.02621).
- [6] V. A. Naumov and D. S. Shkirmanov, Extended Grimus-Stockinger theorem and inverse square law violation in quantum field theory, *Eur. Phys. J. C* **73**, 2627 (2013), [arXiv:1309.1011 \[hep-ph\]](https://arxiv.org/abs/1309.1011).
- [7] S. E. Korenblit and D. V. Taychenachev, Extension of Grimus-Stockinger formula from operator expansion of free Green function, *Mod. Phys. Lett. A* **30**, 1550074 (2015), [arXiv:1401.4031 \[math-ph\]](https://arxiv.org/abs/1401.4031).
- [8] V. A. Naumov and D. S. Shkirmanov, Reactor antineutrino anomaly reanalysis in context of inverse-square law violation, *Universe* **7**, 246 (2021).
- [9] D. V. Naumov, V. A. Naumov, and D. S. Shkirmanov, Inverse-square law violation and reactor antineutrino anomaly, *Phys. Part. Nucl.* **48**, 12 (2017), [arXiv:1507.04573 \[hep-ph\]](https://arxiv.org/abs/1507.04573); Quantum field theoretical description of neutrino oscillations and reactor antineutrino anomaly, *Phys. Part. Nucl.* **48**, 1007 (2017).
- [10] A. N. Ivanov, R. Hollwieser, N. I. Troitskaya, M. Wellenzohn, O. Zhrebtssov, and A. P. Serebrov, Deficit of reactor antineutrinos at distances smaller than 100 m and inverse β -decay, *Phys. Rev. C* **88**, 055501 (2013), [arXiv:1306.1995v2 \[hep-ph\]](https://arxiv.org/abs/1306.1995v2).
- [11] V. Kopeikin, M. Skorokhvatov, and O. Titov, Reevaluating reactor antineutrino spectra with new measurements of the ratio between ^{235}U and ^{239}Pu β spectra, *Phys. Rev. D* **104**, L071301 (2021), [arXiv:2103.01684 \[nucl-ex\]](https://arxiv.org/abs/2103.01684).
- [12] P. Huber, On the determination of antineutrino spectra from nuclear reactors, *Phys. Rev. C* **84**, 024617 (2011), Erratum *ibid. C* **85**, 029901 (2012), [arXiv:1106.0687 \[hep-ph\]](https://arxiv.org/abs/1106.0687).
- [13] Th. A. Mueller, D. Lhuillier, M. Fallot, A. Letourneau, S. Cormon, *et al.*, Improved predictions of reactor antineutrino spectra, *Phys. Rev. C* **83**, 054615 (2011), [arXiv:1101.2663 \[hep-ex\]](https://arxiv.org/abs/1101.2663).
- [14] M. Fallot, S. Cormon, M. Estienne, A. Algora, V. M. Bui, *et al.*, New antineutrino energy spectra predictions from the summation of beta decay branches of the fission products, *Phys. Rev. Lett.* **109**, 202504 (2012), [arXiv:1208.3877 \[nucl-ex\]](https://arxiv.org/abs/1208.3877).